FEBS Letters 350 (1994) 258–262

FEBS 14394

Direct observation of the iron binding sites in a ferritin

Paul D. Hempstead, Aaron J. Hudson, Peter J. Artymiuk*, Simon C. Andrews, Mark J. Banfield, John R. Guest, Pauline M. Harrison

The Krebs Institute, Department of Molecular Biology and Biotechnology, University of Sheffield, Sheffield S10 2UH, UK

Received 16 May 1994; revised version received 7 July 1994

Abstract

X-Ray analysis of the ferritin of *Escherichia coli* (Ec-FTN) and of Ec-FTN crystals soaked in $(NH_4)_2Fe(SO_4)_2$ has revealed the presence of three iron-binding sites per subunit. Two of these form a di-iron site in the centre of the subunit as has been proposed for the 'ferroxidase centres' of human ferritin H chains. This di-iron site, lying within the 4-alpha-helix bundle, resemble those of ribonucleotide reductase, methane monoxygenase and haemerythrin. The third iron is bound by ligands unique to Ec-FTN on the inner surface of the protein shell. It is speculated that this state may represent the nucleation centre of a novel type of Fe(III) cluster, recently observed in Ec-FTN.

Key words: Ferritin; Iron-binding site; Binuclear Fe complex; Iron mineralisation

1. Introduction

The mechanism by which the iron-storage protein, ferritin, stores iron has been the focus of many studies, but direct information on the positions of the iron binding sites has been lacking until now. Ferritin molecules are hollow protein shells, assembled from 24 polypeptide chains related by 432 symmetry [1]. The central cavity has a capacity for up to 4500 Fe(III) atoms which are stored as a ferric oxyhydroxide-phosphate mineral [1]. Depending on the species and on iron loading, the iron-cores of natural ferritins vary in composition from phosphate-free ferrihydrite (approximately $5Fe_2O_3 \cdot 9H_2O$) to that approaching ferric phosphate [1,2]. In vitro studies show that the ferric iron-core is deposited within the protein shell, if iron is presented as Fe(II) [3]. The ability of the protein to catalyse Fe(II) oxidation is well established [4,5], but the catalytic mechanism and the subsequent stages leading to mineralisation are not clearly defined. The use of site-directed mutagenesis has implicated a number of residues in iron-binding [4–7], but one of the reasons for the lack of direct information on iron-binding positions is that crystallisation of mammalian ferritins has always involved metal ions, usually Cd^{2+} or Ca^{2+} [1,8]. Such metals compete with binding of Fe^{2+} or Fe^{3+} ions and thus prevent the unequivocal assignment of their sites. Although the presence of nucleation sites on the cavity surface has also been proposed [3,8–10], their positions are uncertain. This may be due, in part, to lack of alignment between the atomic structures of the mature mineral crystallites and the protein [11].

Mammalian ferritin shells contain two types of polypeptide chain (or subunit) known as H and L. Ferroxidase activity is associated only with H-type chains. The main function of the non-catalytic L chains is probably to promote iron-core nucleation [9,10]. All ferritins of invertebrates, plants and bacteria, so far examined, are of the H-type, as judged from amino acid sequence alignment and, in some cases, from their Fe(II) oxidative ability [12]. Two types of ferritin have been isolated from *Escherichia coli*, a haem-containing 'bacterioferritin' (Ec-BFR) [13] and a conventional ferritin (Ec-FTN) [14]. Both of these resemble mammalian H-chain ferritins [12] and both exhibit ferroxidase activity [14,15]. Although Ec-BFR contains only five of the seven amino acid residues associated with this activity in human H chains, Ec-FTN contains all seven.[12].

Ec-FTN has now been crystallised in the absence of metal ions and its three-dimensional structure determined at high resolution (Hempstead, Hudson, Yewdall, Artymiuk, Andrews, Guest and Harrison, unpublished work). Soaking of these crystals with $(NH_4)_2Fe(SO_4)_2$ solution in air has allowed the identification of three iron-binding sites. These sites and other features of the three-dimensional structure of Ec-FTN are described here and discussed in relation to mechanisms of Fe(II) oxidation and mineralisation in ferritin.

2. Materials and methods

Ec-FTN was isolated from an over-producing strain of *E. coli* JRG2449 as described in [14].

Crystals of Ec-FTN, $1.0 \times 1.0 \times 0.8$ mm, were grown by micro-dialysis at 20°C against 20 mM piperazine-HCl buffer, pH 5.2 containing 0.2 M NaCl. The crystals are in tetragonal space group I4 with dimensions $a = b = 13.0$ nm, $c = 17.3$ nm. Data were collected on an in-house SDMW Area Detector, with CuKα radiation. For iron-binding, crystals were dialysed in air against 20 mM $(NH_4)_2Fe(SO_4)_2$ for 24 h. X-ray data were collected at the SERC Daresbury synchrotron source, 0.89 Å wavelength, using a Mar Research image plate, (Table 1). The structure of Ec-FTN was solved by molecular replacement using six subunits of the human H chain ferritin (HuHF) structure [8] as a starting model. The orientations of the non-crystallographic fourfold axes in the unit

*Corresponding author. Fax: (44) (742) 72-8697.

SSDI 0014-5793(94)00781-0

cell were determined by means of a self-rotation function using POLARRFN [16]. Rigid body refinement and simulated annealing were then performed using XPLOR [17] and conventional refinement was carried out using PROLSQ [18]. The metal sites in the iron- loaded Ec-FTN were located using the program FRODO [19] in a difference electron density map $(3F_{PH} - 2F_P)\exp(i\alpha_{Pcalc})$, where PH indicates Ec-FTN plus iron and P, native Ec-FTN. The structure was refined using TNT [20] (details given in Table 1). Refinement of the native Ec-FTN structure is continuing but iron-binding sites can be unambiguously identified in the difference map. The eighteen iron peaks are in the range 11–7.6 σ, the next highest peak, which corresponds to a misplaced methionine suplhur atom, is at the 4.7 σ level.

3. Results and discussion

The three-dimensional structure of Ec-FTN closely resembles those of other ferritins [1,8]. Its subunit is folded as a four-α-helix bundle with a long loop (external to the shell) linking the C-terminus of helix B and the N-terminus of helix C at opposite ends of the bundle. Like those of mammalian ferritins [1,8], a short fifth helix, E, lies roughly along to the radius vector of the shell with its C-terminus at the cavity surface. The space-group of most previously analysed ferritin crystals is F432 with coincidence of molecular 432 and lattice symmetry. The crystallographic subunit contains a single chain and thus the 24 subunits are crystallographically indistinguishable. In contrast, in the tetragonal unit cell of Ec-FTN (space-group I4) the asymmetric unit contains six chains. These subunits, which are related by non-crystallographic symmetry, are virtually indistinguishable their α-carbon atoms superimposing to within ±0.5 Å. The chain folds of Ec-FTN and HuHF are also strikingly similar (α-carbons superposable to within ±1.1 Å), but there are numerous differences in inter-subunit interactions, as expected from their low amino acid sequence identity (24%). Structural features will be described in detail elsewhere and only those regions pertaining to metal binding sites will be considered here.

Three iron-binding sites (presumably Fe^{3+}) are observed in Ec-FTN, lying within about 7 Å of each other. Electron density for these sites (calculated as the difference between iron-containing and iron-free crystals) is shown in Fig. 1, together with iron ligands and main chain in the immediate neighbourhood of the metal sites. A schematic diagram of the metal sites is shown in Fig. 2.

A striking feature of Fig. 1 is the proximity of the two Fe^{3+} peaks of electron density, A and B, which are 3.8 Å apart (average distance for six subunits). The ligands of Fe_A are Glu-27, Glu-62 and His-65 and those of Fe_B are Glu-62 (a bridging ligand), Glu-107 and Glu-144. Gln-141 is not close enough to bind directly to Fe_A (or to Fe_B), but may be linked through water. The corresponding region of HuHF, which is virtually identical except for residue 144, has been shown to bind two Tb^{3+} ions about 3.1 Å apart [8]. The estimated occupancy of the pair of Fe^{3+} ions in Ec-FTN, Fig. 1, is close to unity, indicating that Fe_A and Fe_B are present in the same subunit. They may be joined through a μ-oxo-bridge (or through OH^- or H_2O), although no electron density suggesting such a bridge is observed. However, this could be due to diffraction effects and the relatively low resolution of the analysis. μ-oxo-bridged Fe(III) dimers have been observed by Mössbauer spectroscopy in HuHF [4,5] and also recently in Ec-FTN [21] as an early product of Fe(II) oxidation. The region of Ec-FTN shown in Fig. 2 contains the seven residues that are highly conserved in ferritin H chains, namely Glu-27, Tyr-34, Glu-61, Glu-62, His-65, Glu-107 and Gln-141. In HuHF this region has been identified as the ferroxidase centre with the acid of site-directed variants [4–7]. Replacements E27A or E107A, or E62K plus H65G, lead to marked loss of both ferroxidase activity and Fe(III) dimer production [4–7]. Substitutions, Y34F and Q141E also lead to lower Fe(II) oxidation rates, but to a less extent than in the above [4,7]. An interesting difference between HuHF and Ec-FTN is that Glu-144 seems to be able to bind to both Fe_B and Fe_C (see below and Fig. 2). Residue 144 is either alanine or serine in the H chains of ferritins from animals and plants.

The studies with HuHF variants outlined above, together with computer modelling, led to the proposal that the catalytic mechanism of Fe(II) oxidation involves oxidation of two Fe(II) atoms with production of hydrogen peroxide [6]. It was suggested that oxidation of a close pair of Fe(II) atoms by a single dioxygen molecule, bound to one of them, may account for the fast oxidation

Table 1
Details of crystallographic analysis

	Resolution (Å)	Reflections measured	Unique reflections measured	Percentage completeness of data	R_{merge}*	R_{ref}**	σ_{bond} (Å)	σ_{angle} (°)
Ec-FTN	2.42	240,964	50,555	90.4	0.096	0.25	0.008	1.5
Ec-FTNF†	2.98	79,474	29,324	99.0	0.090	0.27	0.010	1.9

† Ec-FTNF, crystals soaked in $(NH_4)_2Fe(SO_4)_2$.

* $R_{merge} = \Sigma_h \Sigma_j | I(h)_j - \langle I(h) \rangle | / \Sigma_h \Sigma_j I(h)_j$ summed over all measured reflections.

** R_{ref}, crystallographic residual, $R = \Sigma || F_o | - | F_c || / \Sigma | F_c |$.

The mean fractional isomorphous difference was 0.33. σ_{bond}, σ_{angle}, standard deviation of covalent bonds and bond angles, respectively, at current stage of refinement.

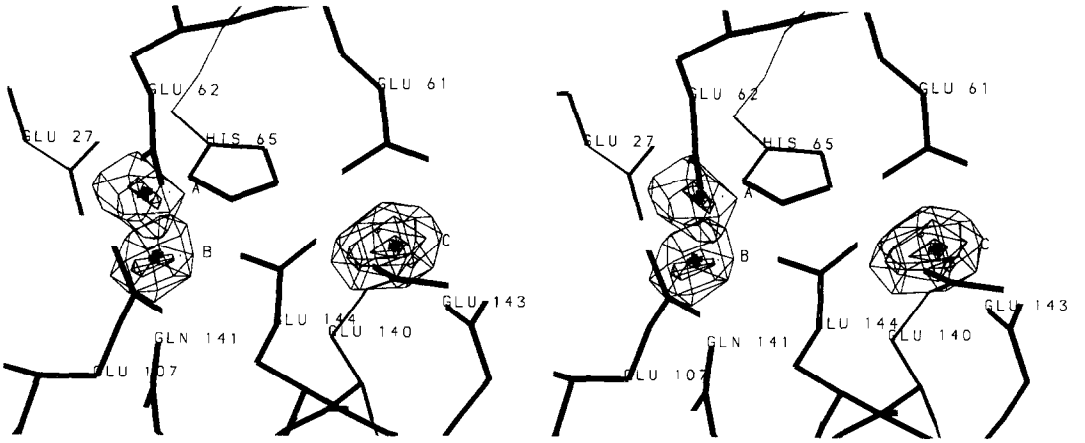

Fig. 1. Part of a subunit of Ec-FTN showing a difference electron density map between iron-containing and iron-free crystals. Three iron-sites A, B and C are shown together with neighbouring side-chains and main chain. The di-iron site, A and B lies in the centre of a subunit and site C lies on the inner surface of the protein shell.

rate. Alternatively oxidation of the two iron atoms may occur sequentially [22], but, in Ec-BFR, an EPR signal has been attributed to an NO-Fe(II) adduct in which NO is bound to a pair of Fe(II) atoms in [23]. The importance of the 'ferroxidase centre' region of ferritin H chains in Fe(II) oxidation has been called into question by the observation that bullfrog L-chain ferritin fails to catalyse oxidation despite the presence of Glu-62 and His-65 [24]. However, there are other substitutions (E27K, E107Q, Q141S) in this region of bullfrog ferritin L chains, which may prevent any iron-oxidative activity [12]. The results of structural analysis given in Figs. 1 and 2 show clearly that Fe atoms do bind in this region of Ec-FTN. The finding of μ-oxo-bridged Fe(III) dimers in Ec-FTN [21], as well as in HuHF [4–7], at very early times after addition of Fe(II) to the apo-proteins, also emphasises the importance of an iron-pair in the oxidative mechanism.

The positions of the two Fe atoms within the 4-helix bundle of Ec-FTN (Fig. 1) are very similar to the observed Tb^{3+} [8] and modelled Fe^{3+} [6] sites of HuHF. Although not shown here, pairs of Tb^{3+} ions also appear in the ferroxidase centre of Ec-FTN, when Ec-FTN crystals are soaked with $TbCl_3$, and these Tb^{3+} ions have the same ligands as those of Fe_A and Fe_B (Banfield, Hempstead, Artymiuk and Harrison, unpublished work). Hence it may be concluded that the modelled iron sites of HuHF are likely to be essentially correct. Mössbauer spectroscopic measurements indicate two slightly different modes of binding. Thus both HuHF and Ec-FTN give two μ-oxo-bridged Fe(III) dimers distinguished by somewhat different Mössbauer parameters [4,5,7,21], due, possibly to variability in the di-iron bridging group (e.g. O^{2-} or OH^-).

The third iron site, Fe_C of Figs. 1 and 2 is different from any metal site observed in HuHF or in horse spleen or rat liver ferritins [1,8]. Of its four ligands, Glu-61, Glu 140, Glu 143 and Glu-144 (in its alternative position), only Glu-61 is conserved in all known 'conventional' ferritins (but not in Ec-BFR). Glu-140 is also present in HuHF and many other ferritins, Glu-144 is unique to the two known FTN sequences. Residue 144 is alanine in mammalian H and leucine in mammalian L chains [12]. The functional significance, of Fe^{3+} at site C is uncertain, although it also has a high occupancy. It is possible that Fe_C is the site of a monomeric Fe(III) species observed in Mössbauer spectra of Ec-FTN [20]. This species is present in a much higher amount in Ec-FTN than Fe(III) monomers in HuHF. Moreover, this Ec-FTN iron behaves differently from the Fe(III) monomers in HuHF under a variety of conditions [21]. Fe_C of Figs. 1 and 2

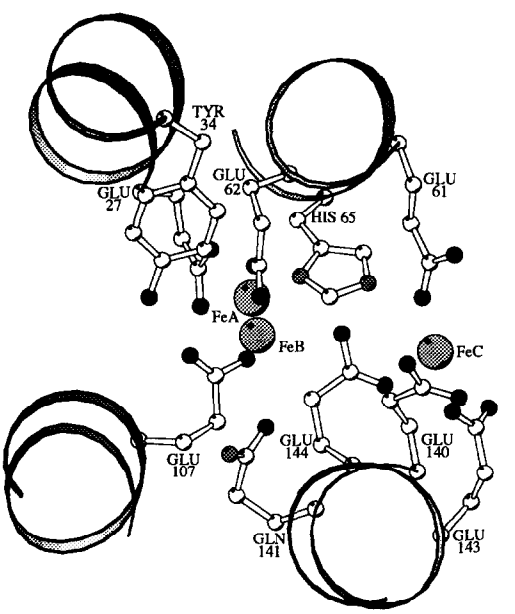

Fig. 2. MOLSCRIPT [29] drawing of the iron sites in Ec-FTN viewed down the axis of the 4-helix bundle. Outside surface of the shell on the left, inside on the right.

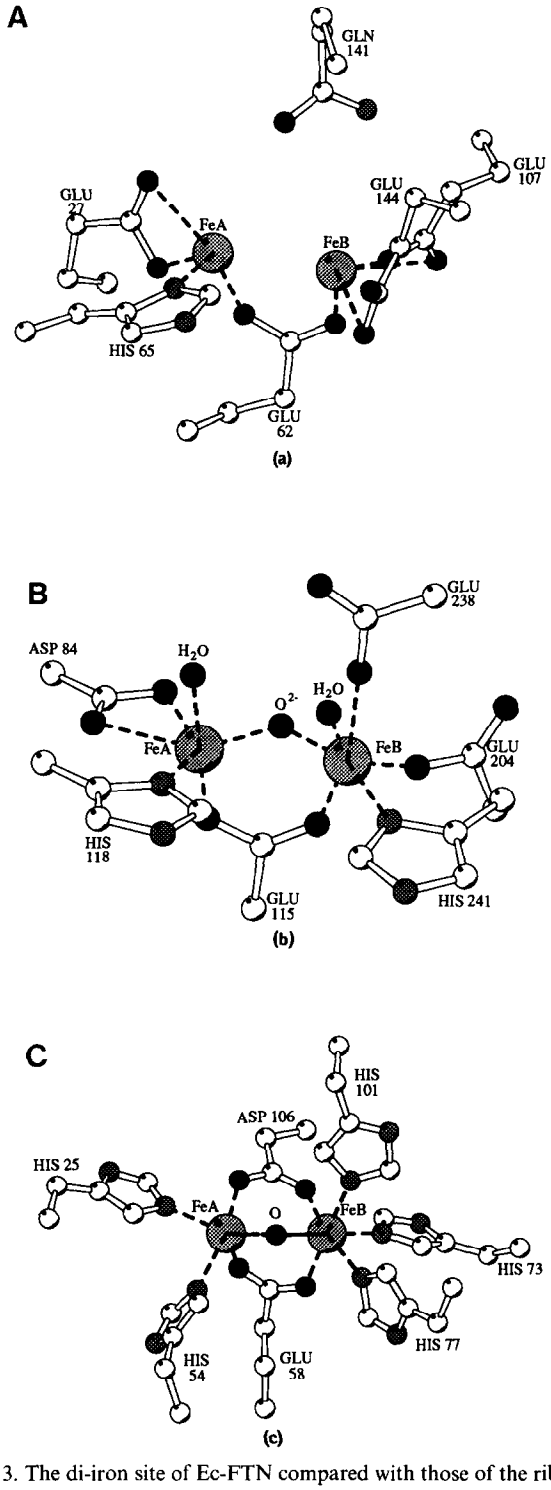

Fig. 3. The di-iron site of Ec-FTN compared with those of the ribonucleotide reductase R2 subunit and haemerythrin. (A) Ec-FTN. Gln-141 cannot bind directly to either FeA or FeB, but may do so through water. (B) R2, is based on a drawing in [24]. (C) Hr is from 2hmq co-ordinates in the Brookhaven Protein Data Bank.

is situated on the inner surface and therefore could, in principle, represent an iron-core nucleation centre. A different nucleation site with ligands not present in Ec-FTN, has been postulated for HuHF [8]. The possibility of a unique nucleation centre is intriguing and could explain another finding of Mössbauer spectral analysis [21]. Subspectra attributed to iron clusters at early stages of iron-core formation are more complex than those of HuHF or of horse spleen ferritin (HoHF) [25]. Unlike HuHF or HoHF in which both magnetic and non-magnetic Fe(III) clusters resemble the mineral ferrihydrite, Ec-FTN exhibits two chemically distinct components, only one of which is ferrihydrite-like. The other is non-magnetic and accounts for about two-thirds of the smaller clusters [21].

Other relevant regions of the Ec-FTN structure are the eight three-fold inter-subunit channels. In crystal structures of HuHF and other mammalian ferritins, metal ions e.g. Ca^{2+}, Cd^{2+}, Zn^{2+} or Tb^{3+}, are found in these channels [1,8]. Mössbauer spectroscopic investigations of site-directed HuHF channel variants have suggested that Fe^{3+} ions can bind in these channels and that they are an entry route for Fe^{2+} [7]. However, the metal ligands Asp-131 and Glu-134 found in the threefold channels of HuHF and other ferritins are replaced, in Ec-FTN, by asparagine and glutamine respectively. No Fe^{3+} or Tb^{3+} ions are found in Ec-FTN channels, implying that such sites are not essential for iron-storage in irrespective of any role they may play in other ferritins.

The X-ray analysis of the Fe-containing derivative of Ec-FTN, together with the spectroscopic studies of iron-binding to HuHF and Ec-FTN described above, establish that μ-oxo-bridged Fe(III) dimers form within the 4-helix bundles of ferritin H chains at the sites depicted in Fig. 2. It is interesting to compare these dimers and their ligands with those of the ribonucleotide reductase R2 component [26] and methane mono-oxygenase (MMO) [27] (which closely resemble each other) and of haemerythrin (Hr) [28], Fig. 3. Ligands of Fe_A are similar to those of the corresponding Fe atom of MMO amd R2. They are on the same side of helix B with the bridging glutamate (Glu-62) and histidine ligand (His-65) in the sequence Glu-X-X-His as found in the other di-iron proteins [26–28]. In Hr the corresponding ligands are spaced by three intervening residues and appear in reverse order His-X-X-X-Glu. Fe_B (Fig. 2) has three amino acid ligands, bridging ligand Glu-62, Glu-107 and Glu-144 (absent from other species), with no histidines, unlike the corresponding Fe atom of MMO (and R2) where the sequence Glu-X-X-His again relates two of its ligands. Fe_B has four amino acid ligands (including the glutamate bridge) in MMO and R2, and five in Hr (glutamate and aspartate bridges and three histidines). It is possible that in Ec-FTN Glu-61 could swing into an alternative position to become a third ligand of Fe_B, as found for Tb_B in HuHF [8]. However, there is no indication in the Ec-FTN electron density map for such alternative conformations. The unique design of the di-iron site in H chain ferritins, with its relative ligand paucity, may reflect the fact that Fe is the substrate, not part of the

binding site of another substrate, and that it must be able to leave the catalytic site after oxidation [4,8]. It is conceivable that only one Fe atom is released from the ferroxidase site to move into the cavity for iron-core formation and that the other Fe atom remains. Such a possibility has been envisaged for Ec-BFR [15].

Acknowledgements: We thank the SERC Protein Engineering Initiative, and the EC BRIDGE Programme (BIOT-CT91–0262). P.J.A. is a Royal Society University Research Fellow. We acknowledge use of the SERC Daresbury Synchrotron Radiation Source and of the CCP4 program suite.

References

[1] Harrison, P.M., Andrews, S.C., Artymiuk, P.J., Ford, G.C., Guest, J.R., Hirzmann, J., Lawson, D.M., Livingstone, J.C., Smith, J.M.A., Treffry, A. and Yewdall, S.J. (1991) Adv. Inorg. Chem. 36, 449–486.

[2] Mann, S., Bannister, J.V. and Williams, R.J.P. (1986) J. Mol. Biol. 188, 225–232.

[3] Macara, I.G., Hoy, T.G., and Harrison, P.M. (1972) Biochem. J. 126,151–162.

[4] Bauminger, E.R., Harrison, P.M., Hechel, D., Nowik, I. and Treffry, A. (1991) Biochim. Biophys. Acta 1118, 48–58.

[5] Bauminger, E.R., Harrison, P.M., Hechel, D., Hodson, N.W., Nowik, I., Treffry, A. and Yewdall, S.J. (1993) Biochem. J. 296, 709–719.

[6] Treffry, A., Hirzmann, J., Yewdall, S.J. and Harrison, P.M. (1992) FEBS Lett. 302, 108–112.

[7] Treffry, A., Bauminger, E.R., Hechel, D., Hodson, N.W., Nowik, I., Yewdall, S.J. and Harrison, P.M. (1993) Biochem. J. 196, 721–728.

[8] Lawson, D.M., Artymiuk, P.J., Yewdall, S.J., Smith, J.M.A., Livingstone, J.C., Treffry, A., Luzzago, A., Levi, S., Arosio, P., Cesareni, G., Thomas, C.D., Shaw, W.V. and Harrison, P.M. (1991) Nature 349, 541–544.

[9] Wade, V.J., Levi, S., Arosio, P., Treffry, A., Harrison, P.M. and Mann, S. (1991) J. Mol. Biol. 221, 1443–1452.

[10] Levi, S., Yewdall, S.J., Harrison, P.M., Santambrogio, P., Cozzi, A., Rovida, E., Albertini, A. and Arosio, P. (1992) Biochem. J. 228, 591–596.

[11] Fischbach, F.A., Harrison, P.M. and Hoy, T.G. (1969) J. Mol. Biol. 39, 235–238.

[12] Andrews, S.C., Arosio, P., Bottke, W., Briat, J.-F., von Darl, M., Harrison, P.M., Laulhère, J.-P., Levi, S., Lobreaux, S. and Yewdall, S.J. (1992) J. Inorg. Biochem. 47, 161–174.

[13] Yariv, J., Kalb, A.J., Sperling, R., Bauminger, E.R., Cohen, S.G. and Ofer, S. (1981) Biochem. J. 197, 171–175.

[14] Hudson, A.J., Andrews, S.C., Hawkins, C., Williams, J.M., Izuhara, M., Meldrum, F.C., Mann, S., Harrison, P.M. and Guest, J.R. (1993) Eur. J. Biochem. 218, 985–995.

[15] LeBrun, N., Wilson, M.T., Andrews, S.C., Guest, J.R., Harrison, P.M., Thomson, A.J. and Moore, G.R. (1993) FEBS Lett. 333, 197–202.

[16] CCP4, Collaboration Computional Project No 4, SERC Daresbury Laboratory, Warrington, UK.

[17] Brünger, A.T. (1989) Acta Cryst. A45, 42–50.

[18] Hendrickson, W.A. and Konnert, J.H. (1980) in: Computing in crystallography (Diamond, R. et al. eds.) pp. 13.01 –13.23, Indian Academy of Sciences, Bangalore, India.

[19] Jones, T.A. (1985) Methods Enzymol. 115, 157–171.

[20] Tronrud, D.E., Ten Eyck, L.F. and Matthews, B.W. (1987) Acta Cryst. A43, 689–501.

[21] Bauminger, E.R., Treffry, A., Hudson, A.J., Hechel, D., Hodson, N.W., Andrews, S.C., Levi, S., Nowik, I., Arosio, P., Guest, J.R. and Harrison, P.M. (1994). Biochem. J. in press

[22] Sun, S. and Chasteen, N.D. (1992) J. Biol. Chem. 267, 25160–25166.

[23] LeBrun, N.E., Cheesman, M.R., Thomson, A.J., Moore, G.R., Andrews, S.C., Guest, J.R. and Harrison, P.M. (1993). FEBS Lett. 323, 261–266.

[24] Waldo, G.S., Ling, J., Sanders-Loehr, J. and Theil, E.C. (1993) Science 259, 796–798.

[25] Bauminger, E.R., Harrison, P.M., Nowik, I. and Treffry A. (1989) Biochemistry 28, 5486–5493.

[26] Nordlund, P., Sjöberg, B.-M. and Eklund, H. (1990) Nature 345, 593–598.

[27] Rosenweig, A.C., Frederick, C.A., Lippard, S.J. and Nordlund, P. (1993) Nature. 366, 537–543.

[28] Holmes, M.A. and Stenkamp, R.E. (1991) J. Mol. Biol. 220, 723–737.

[29] Kraulis, P.J. (1991) J. Appl. Cryst. 24, 946–950.